Mechanics of Materials 202 (2025) 105252

Contents lists available at ScienceDirect

Mechanics of Materials

journal homepage: www.elsevier.com/locate/mecmat

Research paper

On the dynamic JKR adhesion problem

M. Ciavarella [a,b,*], M. Tricarico [a], A. Papangelo [a,b]

[a] Politecnico di BARI. DMMM department., Viale Gentile 182, 70126 Bari, Italy
[b] Hamburg University of Technology, Department of Mechanical Engineering, Am Schwarzenberg-Campus 1, 21073 Hamburg, Germany

ARTICLE INFO

Invited Editor Ghatu Subhash

Keywords:
Adhesion
Pull-off
Shui model
Dynamic adhesion
JKR model
Viscoelasticity

ABSTRACT

Shui et al. (2020) have recently shown that applying high-frequency vibrations, we can increase the mean adhesion between viscoelastic solids. This is due to the fact that oscillating contact area leads to an effect of increased apparent surface energy during the retraction phase which can be described by the well known empirical Gent and Schultz law (GS). However, Shui et al solution surprisingly appears not to depend on GS constants, which would imply perhaps no amplification. Yi et al. (2024) have made similar experiments, and proposed a simpler fitting model, which seems to work however with widely different GS constant when changing the sphere radius. Here, we solve the JKR dynamic adhesion problem for a sphere oscillating on a substrate by imposing an harmonic oscillation of the contact area, which permits to obtain a very simple solution by simply averaging the resulting cycle of indentation. We find that the solution is close to a JKR form for the mean indentation vs mean force, which we find in a simple approximation. Although there is saturation in the amplification when the contact radius shrinks to zero and the problem becomes that of impacts at large amplitudes of vibrations, experiments show that other saturations occurs first, presently unclear. We discuss also the influence of resonances. We find reasonable agreement with experiments conducted on PDMS.

1. Introduction

The adhesive behavior of soft materials like polymers and silicones is attracting interest in the engineering community particularly for the application in the field of soft robotics (Laschi and Cianchetti, 2014; Sanchez et al., 2023), wearable robots (Proietti et al., 2023), grasping technologies (Giordano et al., 2024), reversible adhesives (Kroner et al., 2010), bio-mechanics (Li et al., 2019), tactile perception (Felicetti et al., 2022). Soft (complaint) materials are inherently safe for humans to interact with and this has pushed the research in the field, envisioning a world where robots could collaborate and interact with humans on daily bases. Interaction with humans requires soft end-effectors capable of manipulating and grasping everyday life objects, by means of controlling the force exerted by the manipulator itself without the risk to cause damage. This has led to several strategies, e.g. electro-adhesive pads (Mastrangelo et al., 2023) or mechanochromic polymers able to change color when a critical stress is achieved (Giordano et al., 2024). There still remains the difficulty of regulating the adhesion force in a way that is fast and efficient, ideally along a wide range of tackiness.

Dynamic adhesion has been suggested as a new mechanism to control the adhesive force and hence manipulation objects as possibly useful in many applications, like space technology, flexible electronics, robotics, and bio-integrated devices. Shui et al. (2020) have demonstrated a robust and predictable method using a viscoelastic PDMS substrate attached to a rigid object (a glass sphere) finding an apparent adhesion enhancement of 77 times for a certain optimal amplitude of vibration and a weakening effect for larger amplitudes. One of the interesting features is that the switching timescale is fast and comparable to that of geckos (15 ms), and that the adhesion switching remains unaffected for more than 2×10^7 vibrations without degradation. To understand the method, it is crucial to understand the role of different parameters, including size, actuation amplitude/frequency, surface roughness, and material properties, and this relies so far mainly on experimental evidence, since a predictive model is lacking.

The possibility to model the mechanism relies on the dependence of the work of adhesion on peeling velocity. Gent-Schultz (GS in the following, 1972) noticed that the surface adhesion (which is w_0 in adiabatic reversible conditions) can increase with crack speed in peeling, and Greenwood (2004) demonstrated that it decreases in healing, leading to the very non linear law

$$w(\dot{a}) = w_0 \left(1 + C\left(-\dot{a}(t)\right)^n\right) \quad \text{for } \dot{a}(t) < 0 \tag{1}$$

$$= w_0 / \left(1 + C\dot{a}(t)^n\right) \quad \text{for } \dot{a}(t) > 0 \tag{2}$$

where C, n are found empirically but seem rather independent on the system's geometry if we believe Maugis–Barquins's experiments on flat

* Corresponding author at: Politecnico di BARI. DMMM department., Viale Gentile 182, 70126 Bari, Italy.
E-mail address: Mciava@poliba.it (M. Ciavarella).

https://doi.org/10.1016/j.mechmat.2025.105252
Received 9 October 2024; Received in revised form 22 November 2024; Accepted 3 January 2025
Available online 15 January 2025

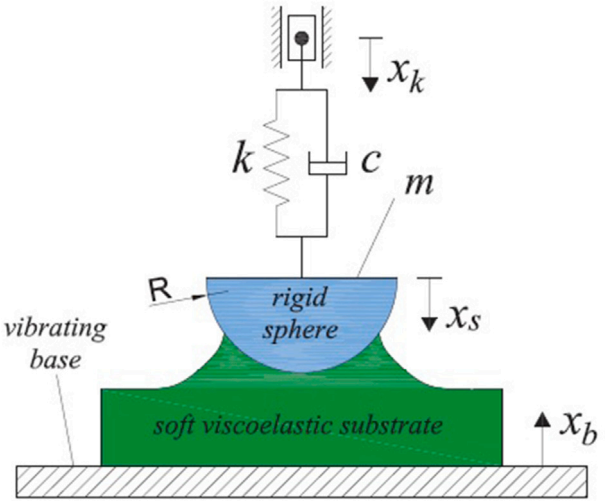

Fig. 1. The Shui et al. (2020) experiment and reference systems.

punch, sphere and peeling (Maugis and Barquins, 1978). We can also write $C = 1/v_0^n$ to obtain a reference speed v_0 which corresponds to amplification 2.

In Shui et al. (2020)'s setup (described in Fig. 1), a base with a viscoelastic carpet is oscillating and puts in vibration a rigid sphere which in turn is pulled by a force via a rubber band spring.

Shui et al. (2020) derive an extension of the well known JKR system of equations (Johnson et al., 1971) for the adhesive quasi-static contact of a sphere, which is ($F > 0$ when compressive)

$$\frac{Ka(t)}{2}\left(3\delta(t) - \frac{a(t)^2}{R}\right) + m\ddot{\delta}(t) + c\dot{\delta}(t) = F(t) \tag{3}$$

$$\frac{3K}{8\pi a(t)}\left(\delta(t) - \frac{a(t)^2}{R}\right)^2 = w\left(\dot{a}(t)\right) \tag{4}$$

where K is an elastic constant of the viscoelastic carpet (in relaxed conditions, or anyway at a frequency corresponding to the indentation frequency), a is contact area radius, F is contact force and δ the contact indentation, i.e. the remote approach between the base and the sphere. Finally, R is sphere radius, m is the sphere mass, and the work of adhesion GS is described by the GS law above ((1),(2)). However, in the process of solution, Shui et al. (2020) find a final equation which gives the mean force as function of the base oscillation amplitude X_b and frequency ω which does not seem to depend on the GS constant as (their Eq. (3)) (subscript "m" indicates mean value)

$$F_m = K\frac{a_m^3}{R} - \sqrt{6\pi w_0 K a_m^3} - \frac{3}{2}\frac{m\omega^2 X_b K a_m}{\sqrt{\left(3Ka_m/2 - m\omega^2\right)^2 + c^2\omega^2}} \tag{5}$$

which could be plotted parametrically varying a_m to find the pull-off (minimum) load. We find this result surprising, since there must be dependence on the GS constants, as indeed we shall find in the present paper.[1]

On the other hand, Shui et al. (2020) experimental results suggest that pull-off amplification is maximum for a certain base oscillation (of about 40 μm in their typical range) and then decays, and they suggested that this is due to a saturation in the GS law deviating from the power law form and perhaps decaying with speed at large speeds. The amplification has also a frequency dependence in that it seems to be saturated for even very small base oscillation if frequency is around 400 Hz, suggesting this is a possible resonance of the system.

Yi et al. (2024) obtain with a similar setup similar experimental results, except for some details: the amplification seems one order of magnitude smaller despite on similar material, and they seem to find a weakening effect of adhesion at very small base oscillations. They propose a very simple model in which the Hertzian load is superposed on an adhesive assumed as

$$F_{adh} = w\left(\dot{a}(t)\right)\frac{d\pi a^2}{d\delta} \tag{8}$$

where various approximations are made namely using Hertz equations (namely $a = \sqrt{R\delta}$) to relate a with $\delta = \delta_m + \delta_A \sin(\omega t)$ gives $\frac{da}{dt} = \frac{da}{d\delta}\frac{d\delta}{dt} = \frac{\sqrt{R}}{2}\frac{\delta_A\cos(\omega t)}{\sqrt{\delta_m+\delta_A\sin(\omega t)}}$ and then plugging this into the GS equations above ((1),(2)). It is assumed $\delta_m = \delta_A$ so that there is no real search for the pull-off condition, and the resulting force is integrated in time to find the mean value. However, it is evident from the results that the GS constant which fits the results vary widely when changing the sphere radius of small amounts and appear also outside the common range where $n < 1$, which suggests the solution is a fit, but the GS constants are not the true constants which must be unique for a given interface.

An alternative solution is therefore proposed here, stemming form the fact that the strong non linearity and difficulty in relating the contact area oscillation with the work of adhesion variations and the indentation oscillations can be simplified if one starts with an "virtual" input of the contact area variation. We then find an exact solution by simply numerically obtain the cycle of oscillation of indentation via one of the JKR dynamic equations, and the mean force from the average of the other JKR equation. This permits to reveal the relation between mean force and mean contact area, which leads to pull-off when the force is minimum. We find that the shape of the force-area curve continues to resemble a JKR shape, and we find an approximate solution guided by some reasonable estimate on mean and amplitude of the indentation cycle: we find however that the resulting "dynamic JKR curve" needs a corrective factor on the product $\omega\delta_A$, which we tested with extensive variation of parameters on the GS law since we dispose of the exact numerical solution, and then we show detailed results of the exact and the approximate solution for a set of constants relative to some experiments which we briefly described on our own setup very similar to the Shui et al. (2020) one. In the next step, we observe that outside from resonance, the indentation oscillation is coincident with the base amplification oscillation.

2. The oscillating contact area

Since most of the trouble in solving the problem come from the GS law in the contact radius velocity, we assume the area is an harmonic oscillation

$$a(t) = a_m + a_A \sin(\omega t) \tag{9}$$

where generally $a_A \ll a_m$. To attempt to model the case when contact is lost and there are impacts (which result in a more complicated problem), we also consider the case where $a_A > a_m$, in which case we take a truncated oscillation when $a(t) \geq 0$. In the cases when $a(t) = 0$ the contact force is obviously zero and $\delta(t)$ is not predicted by the contact equations, but perhaps forced externally.

We are neglecting the slow unloading rate in the contact which may affect results, but which will be harder to take into account since it will make the problem non periodic.

[1] Shui et al. (https://www.researchgate.net/publication/386115815) have recently clarified that their damping factor c really should be considered to depend on the GS constants, because it is a system's parameter which should be measured. However, their predicted pull-off (Eq.16 of Supplementary Info)

$$F_{m,po} = -m\omega^2 X_b\sqrt{1 + \frac{m\omega^2}{c^2}} \tag{6}$$

which can fit anything except the values of pull off less than that obtained for infinite c which is

$$F_{m,po} = -m\omega^2 X_b \tag{7}$$

It turns out in our case we find pull-off is indeed much less than this limit, showing their method is flawed.

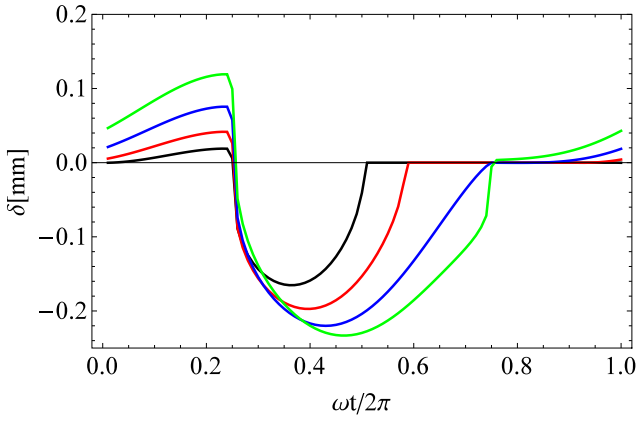

Fig. 2. Examples of cycles of exact indentation δ as for sinusoidal oscillation of area for frequency $\omega = 2\pi \times 200$ rad/s where system parameters are $K = 9.33$ MPa, $R = 51$ mm, $w_0 = 240$ mJ/m^2, $C = (1/0.0445)^n$ [(mm/s)$^{-n}$]; $n = 0.531$. Black, red, blue, green curves correspond to $a_m = 33, 500, 1000, 1500$ μm while a_A =1 mm in all cases. (For interpretation of the references to color in this figure legend, the reader is referred to the web version of this article.)

2.1. Exact solution for δ

We find for a given cycle of contact area variation (hence for a triplet ω, a_m, a_A), from GS law above ((1), (2)), the instantaneous work of adhesion, and hence from (4) we find the cycle of $\delta(t)$ exactly in the steady state. An example of this cycle is reported in Fig. 2 , for various conditions, namely black, red, blue, green curves correspond to $a_m = 33, 500, 1000, 1500$ μm while $a_A = 1$ mm in all cases. Hence, black and red curves are extreme cases where we have a large interval when the indentation is set to zero according to the contact Eq. (4), while blue and green curves are cases where contact is never lost. All system's parameters are defined in Fig. 2 legend, and correspond to experimental parameters in our system, as we shall describe later.

We notice that maxima and minima of indentation oscillation occur near $\pi/2$ and π, respectively, in cases where contact is not lost and amplitude of area oscillation is not large. This will be the basis of an estimate which we describe in the next paragraph, which leads to a JKR solution, which we then correct empirically to have a simple approximate solution to have a ready-to-use formula as an alternative to the exact methodology we are describing.

After obtaining the exact cycle of $\delta(t)$, we can average the result and obtain the mean value δ_m. We can use the second of the JKR governing Eqs. (3), to get the force. Indeed, the average force for any a_A results in cancellation of all the dynamics terms since there is no mean velocity nor mean acceleration. For small $a_A < a_m$, we could get an approximation as

$$F_m(\omega, a_m, a_A) = \frac{K a_m}{2}\left(3\delta_m(\omega, a_m, a_A) - \frac{a_m^2}{R}\right) \tag{10}$$

but we do not resort to this and compute numerically the mean force as the corresponding $F_m(\omega, a_m, a_A)$ from the full (3) and for each fixed ω, a_A for example, we obtain the resulting curve for $F_m(a_m)$ from which it is easy to find the minimum corresponding to pull-off. We record also the area where pull-off is found as $a_{m,po}$. Notice that when we impose in the harmonic formula (9) with $a_A > a_m$, we compute a_m a posteriori for the non harmonic imposed cycle with $a(t) \geq 0$. Similarly, during instants in which $a(t) = 0$, we consider $\delta(t) = 0$ as this leads to zero contact force during these instants, and hence the results are consistent to the averaging leading to the main result of Eq. (10). These details about possible loss of contact and impact however are not going to be relevant for our simulations, since they occur outside the range observed.

2.2. Estimate for δ and a JKR approximate result

We have seen that under the assumption $a_A \ll a_m$ the peak indentation δ occurs when the contact area is largest and the minimum indentation when the contact area is the mean value. We have obviously $a_{\pi/2} = a_m + a_A$ and $a_\pi = a_m$ and we write the instantaneous work of adhesion in these time instants

$$w_{\pi/2} = w_0 \tag{11}$$

$$w_\pi = w_0\left(1 + C\left(a_A\omega\right)^n\right) \tag{12}$$

Using one of the JKR equations (Johnson et al., 1971) for $\delta(t)$, namely (4)

$$\delta(t) = \frac{a(t)^2}{R} - \sqrt{\frac{8\pi}{3K}\left(a_m + a_A\sin(\omega t)\right)w(t)} \tag{13}$$

we get

$$\delta_{\pi/2} = \frac{\left(a_m + a_A\right)^2}{R} - \sqrt{\frac{8\pi}{3K}a_m w_0} \tag{14}$$

$$\delta_\pi = \frac{a_m^2}{R} - \sqrt{\frac{8\pi}{3K}a_m w_0\left(1 + C\left(a_A\omega\right)^n\right)} \tag{15}$$

Hence, a (very crude) estimate of the mean indentation and of the amplitude for $a_A < a_m$

$$\delta_m = \frac{\delta_{\pi/2} + \delta_\pi}{2} = \frac{a_m^2}{R} - \frac{1}{2}\left(\sqrt{\frac{8\pi}{3K}a_m w_0\left(1 + C\left(a_A\omega\right)^n\right)} + \sqrt{\frac{8\pi}{3K}a_m w_0}\right) \tag{16}$$

$$\delta_A = \frac{\delta_{\pi/2} - \delta_\pi}{2} = \frac{a_m a_A}{R} + \frac{1}{2}\left(\sqrt{\frac{8\pi}{3K}a_m w_0\left(1 + C\left(a_A\omega\right)^n\right)} + \sqrt{\frac{8\pi}{3K}a_m w_0}\right) \tag{17}$$

Now we can use the second of the JKR governing Eqs. (3), in the averaged approximate from Eq. (10), to get the mean force using our approximate result for δ_m, (16), obtaining exactly a JKR solution for the mean quantities

$$F_m = K a_m\left(\frac{a_m^2}{R} - 3\sqrt{\frac{2\pi}{3K}w_{eff}a_m}\right) \tag{18}$$

where

$$w_{eff} = \frac{w_0}{4}\left(\sqrt{1 + C\left(a_A\omega\right)^n} + 1\right)^2 \tag{19}$$

The minimum of this follows the JKR pull-off contact radius

$$a_{mpo} = \left(\frac{3\pi R^2}{2K}w_{eff}\right)^{1/3} \tag{20}$$

and therefore results in a minimum at pull-off which is

$$F_{m,po} = -\frac{3}{2}\pi R w_{eff} = -\frac{3}{2}\pi R\frac{w_0}{4}\left(\sqrt{1 + C\left(a_A\omega\right)^n} + 1\right)^2 \tag{21}$$

Notice that this solution leads to the classical JKR solution for no amplitude i.e. no oscillation. We can also rewrite δ_m, δ_A in terms of w_{eff}

$$\delta_m = \frac{a_m^2}{R} - \sqrt{\frac{8\pi}{3K}a_m w_{eff}} \tag{22}$$

$$\delta_A = \frac{a_m a_A}{R} + \sqrt{\frac{8\pi}{3K}a_m w_{eff}} \tag{23}$$

It turns out that this solution needs an empirical corrective factor β in reducing the speed for the effective work of adhesion to be a reasonable approximation, namely

$$w_{eff,corr} = \frac{w_0}{4}\left(\sqrt{1 + C\left(\frac{a_A\omega}{\beta}\right)^n} + 1\right)^2 \tag{24}$$

where we found $\beta \approx 2.5$. Fig. 3(a) shows some results for the mean force vs mean indentation curves obtained exactly (solid black, blue, red correspond to $a_A = 250, 500, 750$ μm), for frequency $\omega = 2\pi \times 400$ rad/s for system parameters as Fig. 2, and dashed line is our approximate solution (18) with corrected effective work of adhesion (24) with $\beta = 2.5$. As it is clear, for very large amplitudes of the area oscillation (consider that the mean value is around 2 mm in most cases near pull-off), there is significant deviation from our JKR approximate result, but otherwise it is a reasonable and useful approximation. The optimal corrective factor β was found by minimizing the error of effective work of adhesion (more precisely, the pull-off value obtained from the full algorithm we described vs the approximate result (24)) across a large range of possible n parameters ($n = 0.1 - 0.9$) and ratio of velocities $v_{\max}/v_0$ where $v_{\max}$ is the peak velocity of contact area oscillation, and v_0 the other GS constant. Indeed, Fig. 3(b) shows the ratio of the exact vs approximate amplification of pull-off over a wide range of $v_{\max}/v_0$ spanning all decades from zero to $v_{\max}/v_0 = 100$, and n coefficients ($n = 0.1, 0.3, 0.5, 0.7, 0.9$ for black, red, blue, black dashed and red dashed curves, respectively). As it can be seen the error becomes significant only for very large velocities, where in general the physical problem show saturation before the solution becomes inaccurate anyway.

The mean contact area radius at pull off a_{mpo} as function of the amplitude of oscillation of contact radius a_A is plotted next in Fig. 4. Here, solid black, blue, red correspond to the exact results for frequency $\omega = 2\pi\times200, 2\pi\times300, 2\pi\times400$ rad/s for system parameters as Fig. 2, and dashed line is our approximate solution (20) with corrected effective work of adhesion (24) with $\beta = 2.5$. As it can be seen, the approximation for the highly non linear curve is effective, but in numerical results there are some more complex trends, like the crossing between the black and the blue curve and the decaying trend results at very large oscillations. The discrete nature of the exact results stems from the numerical discretization.

Next, we plot in Fig. 5 the mean contact indentation at pull-off, as a function of amplitude of oscillation of contact radius a_A. Here, solid black, blue, red correspond to the exact results for frequency $\omega = 2\pi \times 200, 2\pi \times 300, 2\pi \times 400$ rad/s for system parameters as Fig. 2, and dashed line is our approximate solution obtained from the JKR curve with corrected effective work of adhesion (24) with $\beta = 2.5$ at mean contact radius at pull-off as per (20). As it can be seen, the mean contact indentation is negative (meaning the contact operates pulling the two surfaces apart) and the value remains relatively small. The approximation is reasonably good again, with deviations for the largest amplitudes of a_A. The reason this deviation will not affect much results is that in Eq. (10) the value of δ_m does not affect much results, which are close to assuming $\delta_m = 0$ anyway.

In the next figure, Fig. 6, we plot the amplitude of oscillating indentation at pull-off, obtained numerically by estimating the first harmonic amplitude, namely considering

$$\delta_c = \frac{1}{\pi}\int_0^{2\pi} \delta(\tau)\cos(\tau)\, d\tau \tag{25}$$

$$\delta_s = \frac{1}{\pi}\int_0^{2\pi} \delta(\tau)\sin(\tau)\, d\tau \tag{26}$$

$$\delta_A = \sqrt{\delta_c^2 + \delta_s^2} \tag{27}$$

and dashed lines permit the comparison with our approximate solution (23) with (20) with corrected effective work of adhesion (24) with $\beta = 2.5$. Once again, the comparison is satisfactory, considering it is a simple estimate.

We finally move to the quantity of most direct interest, namely, the amplification of pull-off, which we plot in Fig. 7 as a function of the amplitude of oscillation of contact radius a_A. Solid black, blue, red correspond to frequency $\omega = 2\pi\times200, 2\pi\times300, 2\pi\times400$ rad/s for system parameters as Fig. 2, and dashed line is our approximate solution (21) with corrected effective work of adhesion (24) with $\beta = 2.5$.

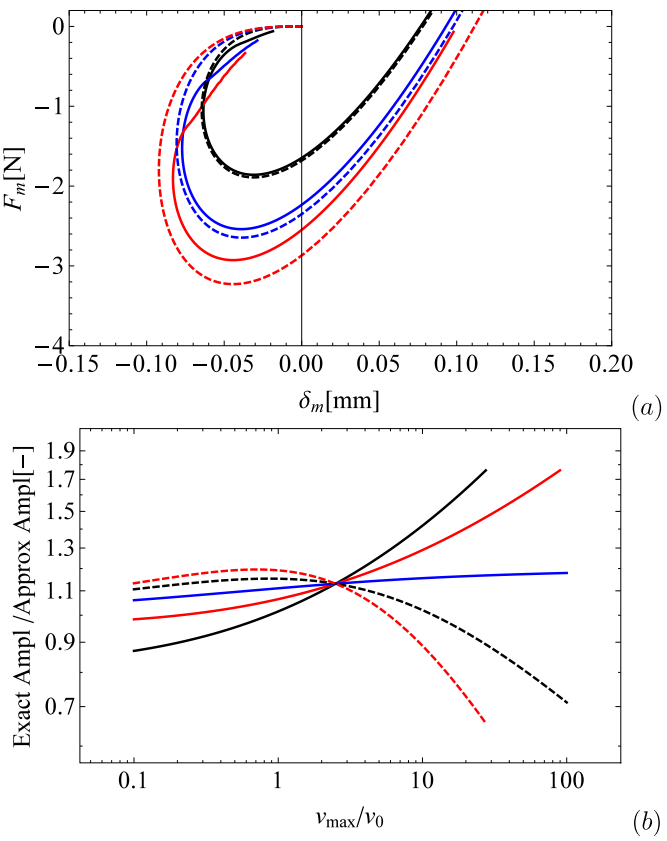

Fig. 3. (a) The mean force mean indentation curve obtained exactly (solid black, blue, red correspond to $a_A = 3/10, 3/5, 9/10$ mm), for frequency $\omega = 2\pi\times400$ rad/s for system parameters as Fig. 2, and dashed line is our approximate solution (18) with corrected effective work of adhesion (24) with $\beta = 2.5$. (b) Exact over approximate amplification of pull-off (ratio of pull-off value obtained from the full algorithm we described over the approximate result obtained with (24)) over a wide range of $v_{\max}/v_0$ spanning all decades from zero to $v_{\max}/v_0 = 100$, and n coefficients ($n = 0.1, 0.3, 0.5, 0.7, 0.9$ for black, red, blue, black dashed and red dashed curves, respectively). (For interpretation of the references to color in this figure legend, the reader is referred to the web version of this article.)

Finally, we provide in Fig. 8 a comparison between amplitude and mean oscillation of indentation at pull off for the usual 3 frequencies, namely exact theory (discrete data points) and our approximate theory.

3. Experimental testing

PDMS samples were prepared using the commercial elastomer Dow Sylgard 184, with a base to curing agent volume ratio of 10:1. The vibrations-regulated adhesion tests were carried out on the customized test rig whose schematics was illustrated in Fig. 1. The PDMS sample (attached to a glass slide), was placed in the middle of a PMMA transparent beam with a rectangular cross section and a thickness of 1 cm. The setup is similar to that in Shui et al. (2020). Real-time images of the contact area were recorded with a high-resolution camera placed under the beam, to extract results for the Gent-Schulz constants under monotonic tests. The loading rate was set to 100 μm/s. At a certain value of preload, a dwell time of 60 s is allowed for stress relaxation. Subsequently, the electrodynamics shakers were manually driven to desired amplitude (by adjusting the amplifier's gain), followed by an additional 60 s dwell time. The sample was then unloaded at 5 μm/s.

The quasi static adhesion tests were performed on the same test rig, but with a rigid link between the load cell and the indenter. Loading and unloading velocities were set to 0.1 μm/s, with 60 s dwell time in between.

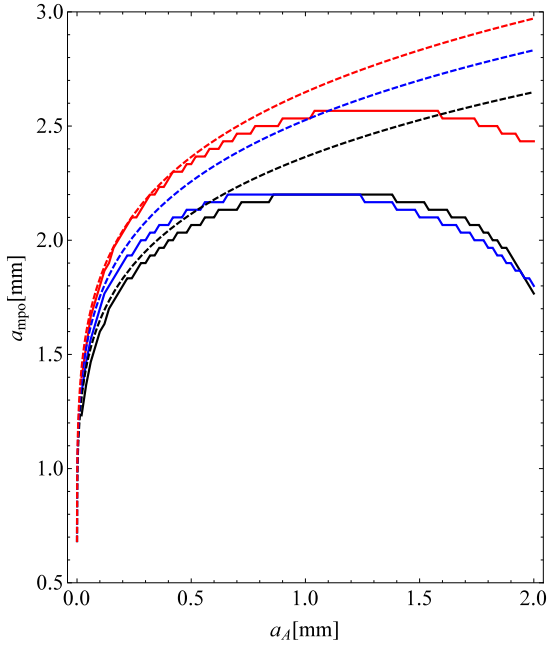

Fig. 4. The mean contact area radius at pull off a_{mpo} as function of the amplitude of oscillation of contact radius a_A. Solid black, blue, red correspond to frequency $\omega = 2\pi \times 200, 2\pi \times 300, 2\pi \times 400$ rad/s for system parameters as Fig. 2, and dashed line is our approximate solution (20) with corrected effective work of adhesion (24) with $\beta = 2.5$. (For interpretation of the references to color in this figure legend, the reader is referred to the web version of this article.)

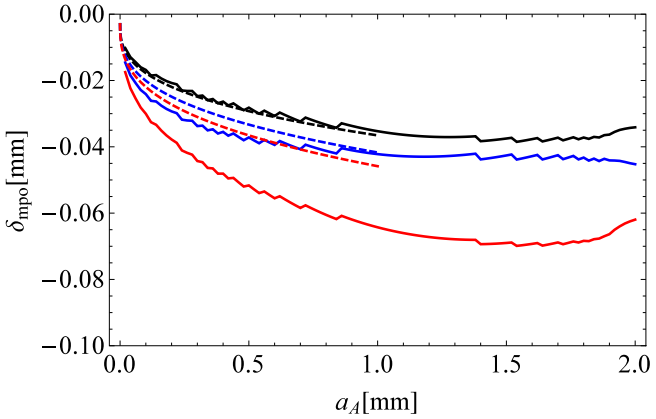

Fig. 5. The mean contact area radius at pull off δ_{mpo} as function of the amplitude of oscillation of contact radius a_A. Solid black, blue, red correspond to frequency $\omega = 2\pi \times 200, 2\pi \times 300, 2\pi \times 400$ rad/s for system parameters as Fig. 2, and dashed line is our approximate solution (22) with (20) with corrected effective work of adhesion (24) with $\beta = 2.5$. (For interpretation of the references to color in this figure legend, the reader is referred to the web version of this article.)

Static (i.e. without vibration) tests were performed to characterize the mechanical response of the PDMS samples (thickness 3 mm). The crack velocity ($v = -da/dt$) in the proximity of pull-off was also measured and correlated to the effective work of adhesion through an empirical Gent-Schultz power law (Gent and Schultz, 1972) (Eq. (1)) where $w_0 = 236$ mJ/m^2 is the quasi-static work of adhesion (found experimentally), and the work of adhesion w was calculated as follows (Ciavarella, 2021)

$$w = \frac{\left(F_H - F\right)^2}{6\pi R F_H} \tag{28}$$

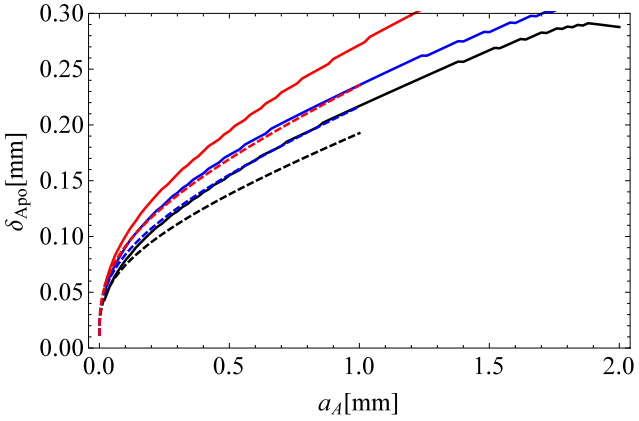

Fig. 6. The amplitude of oscillation of the contact indentation δ_{Apo} at pull-off as a function of the amplitude of oscillation of contact radius a_A. Solid black, blue, red correspond to frequency $\omega = 2\pi \times 200, 2\pi \times 300, 2\pi \times 400$ rad/s for system parameters as Fig. 2, and dashed line is our approximate solution (23) with (20) with corrected effective work of adhesion (24) with $\beta = 2.5$. (For interpretation of the references to color in this figure legend, the reader is referred to the web version of this article.)

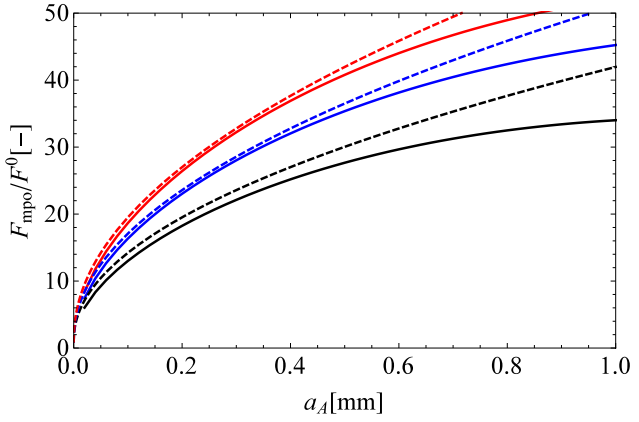

Fig. 7. The amplification of pull-off F_{mpo}/F^0 where $F^0 = -3/2\pi R w_0$ is pull-off in quasi-static conditions, as a function of the amplitude of oscillation of contact radius a_A. Solid black, blue, red correspond to frequency $\omega = 2\pi \times 200, 2\pi \times 300, 2\pi \times 400$ rad/s for system parameters as Fig. 2, and dashed line is our approximate solution (21) with corrected effective work of adhesion (24) with $\beta = 2.5$. (For interpretation of the references to color in this figure legend, the reader is referred to the web version of this article.)

We found $v_0 = 0.0445$ mm/s and $n = 0.531$, which gives the constants used in all the Figures of the present paper. More details about the experiments, and also many more comparison with an alternative full numerical solution of the full dynamic problem are given in Tricarico et al. (2024) where the reader is redirected for more information.

The comparison between experimental amplification and the theory (Fig. 9) (exact and approximate) is relatively satisfactorily, since the results don't depend much on frequency, except at large oscillations. The "exact" theory seems to predict a saturation and perhaps a decay of pull-off but at much larger amplification (of about $F_{mpo}/F^0 = 32$, not shown in the scale, for the smaller frequency), so that another mechanism of saturation is needed to explain the experimental results deviating from the present solution using the power law GS law. Unfortunately the GS experiments were not possible at very large retraction velocities, so that it is not possible to suggest if the saturation is due to saturation in the GS law.

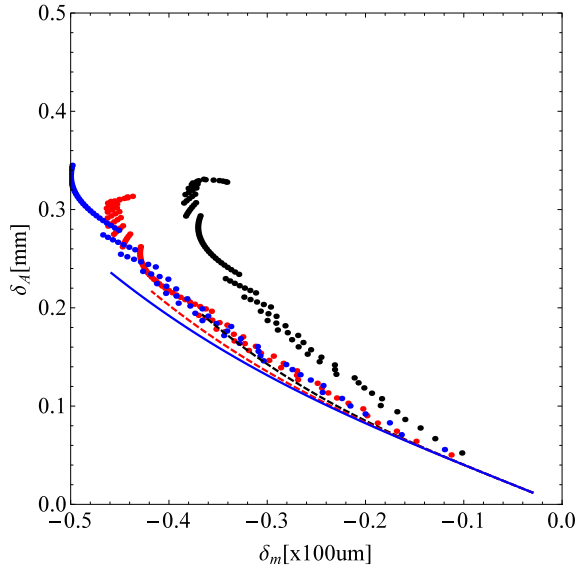

Fig. 8. Amplitude vs mean oscillation of indentation at pull off for the usual 3 frequencies, namely exact theory (discrete data points) and our approximate theory. Black, blue, red markers or lines correspond to frequency $\omega = 2\pi \times 200, 2\pi \times 300, 2\pi \times 400$ rad/s for system parameters as Fig. 2. Corrected effective work of adhesion (24) with $\beta = 2.5$. (For interpretation of the references to color in this figure legend, the reader is referred to the web version of this article.)

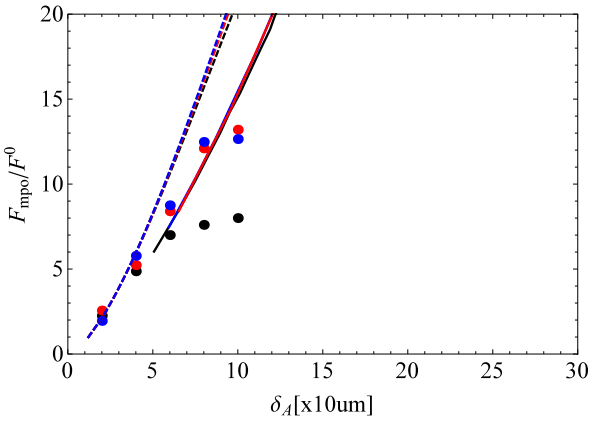

Fig. 9. Experimental results of the dynamic adhesion tests amplification of pull-off load F_{mpo}/F^0, compared with the "exact" theory" with solid lines (with a dynamic modulus estimated as $K = 9.3$ MPa, slightly higher than the relaxed one of 4 MPa): black, blue, red correspond to frequency $\omega = 2\pi \times 200, 2\pi \times 300, 2\pi \times 400$ rad/s for system parameters as all figures in this paper. (For interpretation of the references to color in this figure legend, the reader is referred to the web version of this article.)

According to our estimate (24), an amplification of pull-off of the order of experiments corresponds to

$$v = a_A \omega = 2.5 \left(\frac{\left(48^{0.5} - 1\right)^2 - 1}{1/0.0445^{0.531}} \right)^{1/0.531} = 86 \text{ mm/s} \tag{29}$$

which is just way outside our measured range.

4. Discussion: dynamic effects

The results of the experimental tests we described in the previous paragraph do not depend much on the resonances of the system, since they are relative to 200,300,400 Hz, which are much higher than the resonances in our experimental system. In these conditions, the contact indentation oscillation corresponds to the base oscillation. To understand this, we write the full equations for the system in Fig. 1, to include also the effect of the holding spring. The dynamic equilibrium equation at time t of the spherical indenter reads

$$m\ddot{x}_s + c\dot{x}_s + k(x_s - x_k) = -F + mg \tag{30}$$

where a dot superposed means differentiation with respect to time, i.e. $\dot{x} = dx/dt$, c is a small damping coefficient, F is the force that the substrate applies to the indenter that is considered positive when compressive and $g = 9.807$ m/s^2 is the gravitational acceleration.

The excitation is physically applied through an imposed harmonic vibration of the substrate base which we can assume without loss of generality to be sinusoidal

$$x_b = X_{bs} \sin(\omega t) \tag{31}$$

We assume here that this vibration, applied to the substrate bottom (see Fig. 1), leads to an harmonic indentation

$$\delta = x + x_b = x + X_{bs} \sin(\omega t) \tag{32}$$

In turn, we have already obtained that the contact force resulting from the indentation δ is also harmonic and can be written for $a_A \ll a_m$ (looking at Eq. (3)) as (we write F_s for F_{As} and δ_s for δ_{As} to simplify notation)

$$\begin{aligned} F &= F_m + F_s \sin(\omega t) + F_c \cos(\omega t) \\ &= F_m + \frac{3}{2} K a_m \left(\delta_s \sin(\omega t) - \delta_c \cos(\omega t) \right) \end{aligned} \tag{33}$$

Therefore, the equation of motion for the sphere in terms of contact indentation is

$$\begin{aligned} m\ddot{\delta} + c\dot{\delta} + k\delta = &-m\omega^2 X_{bs} \sin(\omega t) + c\omega \left(X_{bs} \cos(\omega t) \right) \\ &+ k X_{bs} \sin(\omega t) - \frac{3}{2} K a_m \left(\delta_s \sin(\omega t) + \delta_c \cos(\omega t) \right) \end{aligned} \tag{34}$$

Further

$$\delta = \delta_s \sin(\omega t) + \delta_c \cos(\omega t) \tag{35}$$

so equaling the cosine terms in (34)

$$\delta_c = -\frac{X_{bs} c\omega + c\omega \delta_s}{k + \frac{3}{2} K a_m - m\omega^2} \tag{36}$$

and from equaling the sin terms in (34)

$$\frac{\delta_s}{X_{bs}} = \frac{\left(k - m\omega^2\right)\left(k + \frac{3}{2} K a_m - m\omega^2\right) - (\omega c)^2}{\left(k + \frac{3}{2} K a_m - m\omega^2\right)\left(k + \frac{3}{2} K a_m - m\omega^2\right) + (\omega c)^2} \tag{37}$$

so that

$$-\frac{\delta_c}{X_{bs}} = \frac{c\omega}{k + \frac{3}{2} K a_m - m\omega^2} \left(\frac{2k + \frac{3}{2} K a_m - 2m\omega^2}{k + \frac{3}{2} K a_m - m\omega^2 + \frac{(\omega c)^2}{k + \frac{3}{2} K a_m - m\omega^2}} \right) \tag{38}$$

Far from resonance there is small effect of damping, and we obtain the simplified result

$$\frac{\delta_s}{X_{bs}} = \frac{k - m\omega^2}{k + \frac{3}{2} K a_m - m\omega^2} \tag{39}$$

which shows the amplitude of contact oscillation differs from the oscillation imposed to the base because of the effect of contact stiffness.

Hence, collecting results from the contact mechanics study (23), we have that near the resonance (which corresponds to the stiffness of the parallel between the contact stiffness and the spring stiffness), for a given applied oscillation X_b, there will be a large contact indentation oscillation δ_A, and this will give large amplification, unless the oscillation becomes so large as to reduce adhesion again. This is the case for the experiments in Shui et al. (2020). In our experiments we reported in the previous paragraph at 200, 300, 400 Hz, X_b is no different from δ_A (only few % difference).

Conclusions

We have provided a simple numerical method to solve the dynamic contact JKR adhesive problem under oscillating conditions, stemming from an harmonic oscillation of the contact radius, which requires no solution of non linear equations or differential non linear equations. Given an assumption of small oscillations and a simplified estimate of the mean and amplitude of contact indentation, we have found an amplified JKR equation: this requires a corrective factor to produce reasonably accurate results with respect to the "exact" theory, which we have tested extensively to be about $\beta = 2.5$. The value of the analytical approximate result is however obvious as it permits identification of the main parameters ruling the problem at small oscillations of indentation. We find in experiments that there is a saturation mechanism for the amplification at large oscillations which is not captured by the simple model with the simple Gent-Schulz power law for work of adhesion: perhaps there needs to be a decay after a maximum. The exact and approximate theories have been compared with experiments recently conducted on the system in our lab, in the limit of large frequencies far from the system resonance, finding satisfactory agreement. We have pointed out limitations in the previous models of the problem in the literature.

CRediT authorship contribution statement

M. Ciavarella: Writing – review & editing, Writing – original draft, Software, Methodology, Investigation, Formal analysis, Data curation, Conceptualization. **M. Tricarico:** Investigation, Data curation. **A. Papangelo:** Writing – review & editing, Supervision, Project administration, Methodology, Investigation, Funding acquisition, Formal analysis, Conceptualization.

Declaration of competing interest

The authors declare that they have no known competing financial interests or personal relationships that could have appeared to influence the work reported in this paper.

Acknowledgments

M.T., M.C. and A.P. were partly supported by the Italian Ministry of University and Research under the Programme "Department of Excellence" Legge 232/2016 (Grant No. CUP - D93C23000100001). A.P. and M.T. were supported by the European Union (ERC-2021-STG, "Towards Future Interfaces With Tuneable Adhesion By Dynamic Excitation" - SURFACE, Project ID: 101039198, CUP: D95F22000430006). Views and opinions expressed are however those of the authors only and do not necessarily reflect those of the European Union or the]European Research Council. Neither the European Union nor the granting authority can be held responsible for them.

Data availability

No data was used for the research described in the article.

References

Ciavarella, M., 2021. Improved muller approximate solution of the pull-off of a sphere from a viscoelastic substrate. J. Adhes. Sci. Technol. 35 (20), 2175–2183.

Felicetti, L., Chatelet, E., Latour, A., Cornuault, P.H., Massi, F., 2022. Tactile rendering of textures by an electro-active polymer piezoelectric device: mimicking friction-induced vibrations. Biotribology 31, 100211.

Gent, A.N., Schultz, J., 1972. Effect of wetting liquids on the strength of adhesion of viscoelastic material. J. Adhes. 3 (4), 281–294.

Giordano, G., Scharff, R.B.N., Carlotti, M., Gagliardi, M., Filippeschi, C., Mondini, A., et al., 2024. Mechanochromic suction cups for local stress detection in soft robotics. Adv. Intell. Syst. 2400254.

Greenwood, J.A., 2004. The theory of viscoelastic crack propagation and healing. J. Phys. D: Appl. Phys. 37 (18), 2557.

Johnson, K.L., Kendall, K., Roberts, A.D., 1971. Surface energy and the contact of elastic solids. Proc. R. Soc. Lond. Ser. A Math. Phys. Eng. Sci. 324, 301–313.

Kroner, E., Maboudian, R., Arzt, E., 2010. Adhesion characteristics of PDMS surfaces during repeated pull-off force measurements. Adv. Eng. Mater. 12 (5), 398–404.

Laschi, C., Cianchetti, M., 2014. Soft robotics: new perspectives for robot bodyware and control. Front. Bioeng. Biotechnol. 2 (3).

Li, R.L., Russ, J., Paschalides, C., Ferrari, G., Waisman, H., Kysar, J.W., Kalfa, D., 2019. Mechanical considerations for polymeric heart valve development: Biomechanics, materials, design and manufacturing. Biomaterials 225, 119493.

Mastrangelo, M., Caruso, F., Carbone, G., Cacucciolo, V., 2023. Electroadhesion zipping with soft grippers on curved objects. Extreme Mech. Lett. 61, 101999.

Maugis, D., Barquins, M., 1978. Fracture mechanics and the adherence of viscoelastic bodies. J. Phys. D: Appl. Phys. 11 (14), 1989.

Proietti, T., O'Neill, C., Gerez, L., Cole, T., Mendelowitz, S., Nuckols, K., et al., 2023. Restoring arm function with a soft robotic wearable for individuals with amyotrophic lateral sclerosis. Sci. Transl. Med. 15 (681), eadd1504.

Sanchez, V., Mahadevan, K., Ohlson, G., Graule, M.A., Yuen, M.C., Teeple, C.B., et al., 2023. 3D knitting for pneumatic soft robotics. Adv. Funct. Mater. 33 (26), 2212541.

Shui, L., Jia, L., Li, H., Guo, J., Guo, Z., Liu, Y., et al., 2020. Rapid and continuous regulating adhesion strength by mechanical micro-vibration. Nature Commun. 11 (1), 1583.

Tricarico, M., Ciavarella, M., Papangelo, A., 2024. Enhancement of adhesion strength through microvibrations: modeling and experiments. Accept., J. Mech. Phys. Solids arXiv preprint arXiv:2411.03182.

Yi, J., Haouas, W., Gauthier, M., Rabenorosoa, K., 2024. A PDMS/Silicon adhesion control method at millimeter-scale based on microvibration. Adv. Intell. Syst. 2400394.